Vine Robots

©SHUTTERSTOCK.COM/KENTOH

Design, Teleoperation, and Deployment for Navigation and Exploration

By Margaret M. Coad, Laura H. Blumenschein, Sadie Cutler, Javier A. Reyna Zepeda, Nicholas D. Naclerio, Haitham El-Hussieny, Usman Mehmood, Jee-Hwan Ryu, Elliot W. Hawkes, and Allison M. Okamura

Researchers are developing a new class of continuum robots characterized by tip extension, significant length change, and directional control. In this article, we call these *vine robots* because of their similarity to plants in their growth-trailing behavior. Due to their growth-based movement, vine robots are well suited for navigation and exploration in cluttered environments. Until now, however, they have not been deployed outside the lab. There are three features that are key for successful deployment in the field. First is portability. Second is the ability to be guided over long enough distances to be useful for navigation. Third is intuitive human-in-the-loop teleoperation, which enables movement in unknown and dynamic environments. We present a vine robot system that is teleoperated using a custom-designed flexible joystick and camera system, can extend long enough for use in navigation tasks, and is portable for use in the field. We report on the deployment of this system in two scenarios: completion of a soft robot navigation competition and exploration of an archaeological site. The competition course required movement over uneven terrain, past unstable obstacles, and through a small aperture. The archeological site required movement over rocks and through horizontal and vertical turns. The robot tip successfully moved past the obstacles and through the tunnels, demonstrating the capability of vine robots to achieve navigation and exploration tasks in the field.

Digital Object Identifier 10.1109/MRA.2019.2947538
Date of current version: 28 November 2019

1070-9932/20©2020IEEE

Authorized licensed use limited to: Stanford University. Downloaded on April 11,2021 at 23:34:42 UTC from IEEE Xplore. Restrictions apply.

Background

There are various potential robotic applications in which nondestructive exploration of small spaces remains challenging for existing robot design, including inspection [1], search and rescue [2], medicine [3], and archeology [4]. Vine robots can potentially fill this need for robots able to move in highly constrained environments.

Unlike continuum robots that lengthen by extending modules that move relative to the environment until fully emitted [5], [6], vine robots emit new material only at the very tip, which enables lengthening without relative movement between the emitted robot body material and the environment. Extension in this way also enables enormous length change, limited only by the amount of material that can be transported to the tip. This form of extension has been realized by different mechanisms [7], but our focus is on vine robots that lengthen using internal air pressure to pass material through the center of their flexible, tubular bodies and turn it inside out at the tip through a process called *eversion*. Mishima et al. [8] list three benefits of pneumatically everting vine robots for navigation in cluttered environments: flexibility to follow tortuous paths, rigidity to support their own weight while traversing gaps, and the ability to access spaces without moving their body relative to the environment. Tsukagoshi et al. [9] point out two additional benefits of pneumatically everting vine robots: their bodies could be used as conduits to deliver water or other payloads to their tip, and, since their movement is driven completely by air pressure rather than electricity, there is no risk of failing electrical components igniting flammable gases in hazardous environments. Hawkes et al. [10] demonstrate the ability of pneumatically everting vine robots to move with ease through sticky, slippery, and abrasive environments and to grow into useful structures through preformed shapes. We hypothesize that the unique features of vine robots enable the execution of navigation and exploration tasks in ways not achievable by other types of robots. Various proof-of-concept designs have been developed for pneumatically [8]–[11] and hydraulically [12] everting vine robot navigation and exploration systems. Using these proof-of-concept designs as a foundation, we developed a complete vine robot system suitable for deployment in the field for navigation and exploration applications.

In this article, we discuss the following:

- *A complete, portable system for vine robot deployment in the field*. Our vine robot system combines the capabilities of the proof-of-concept designs and is steerable, carries a camera, and grows to an arbitrary length from a compact form factor.
- *A reversible steering vine robot actuator that can be easily manufactured in long formats*. We improve upon the design of the actuator presented in [11] and [13] by creating a body-length steering actuator that can be manufactured by heat sealing and attached to the robot body using double-sided tape.
- *A method of mounting a camera at the tip of a vine robot and managing the camera wire using a rigid cap and zipper pocket*. In contrast to the bulky design presented in [8], the limited-length design presented in [9]–[11], and the wireless design presented in [12], we offer a compact tip camera mount and wire management design that enables vine robot growth from a compact base to an arbitrary length.
- *A method for robust control of vine robot growth speed using a motor to restrict growth*. In contrast to [12], our controller preserves control that would be lost if the motor's speed were faster than the pressure-driven growth speed.
- *A geometric model-based method for teleoperated steering using a custom-designed flexible joystick*. We adapt the teleoperation device presented in [14] and the mapping from desired tip position to actuator pressure presented in [11] and [13] to achieve human-in-the-loop teleoperation.
- *A report on vine robot deployment in two locations: at a soft robot navigation competition and an archeological site*. Moving beyond the demonstrations of vine robots completing navigation tasks in laboratory environments presented in [9]–[11], we deploy vine robots in the field.

Control of the vine robot body's motion is enabled by the mechanical, electrical, and pneumatic components of the base station.

Vine Robot System Requirements

A number of requirements were considered for the design of our vine robot system. These stemmed from basic vine robot functionality, our goal of making a system capable of operating in unpredictable environments, and the specific deployment scenarios for testing the vine robot's ability to achieve navigation and exploration tasks in the field. The following subsections present the details of the specific scenarios as well as a summary of the system's design requirements.

Soft Robot Navigation Competition Scenario

The first deployment opportunity for our vine robot system was the soft robot navigation competition at the IEEE International Conference on Soft Robotics in Livorno, Italy, in April 2018 (RoboSoft 2018). The competition tested capabilities considered fundamental for soft robots, such as "mechanical compliance, delicate interaction with the environment, and dexterity" [15], and provided a way to benchmark the capabilities of different robots. The competition course was based on a mock disaster scenario, where a robot enters a building and navigates challenging terrain both inside and

Authorized licensed use limited to: Stanford University. Downloaded on April 11,2021 at 23:34:42 UTC from IEEE Xplore. Restrictions apply.

outside the building. The 9.5-m-long course consisted of four obstacles: a sand pit, a square aperture, stairs, and a set of unstable cylinders that could easily be knocked over. The competition had a task-completion-based scoring system. The sand pit and the stairs only needed to be crossed to achieve all possible points. The aperture's size was chosen by each team, with smaller apertures relative to the robot's diameter yielding more points when traversed. The unstable cylinders needed to be passed through without knocking over any cylinder to earn the full number of points.

Archeological Exploration Scenario

The second deployment of our vine robot system was for exploration at an archeological site in Chavin, Peru, in July 2018. The site was a monumental center of religion and culture for the ancient Andean civilization that flourished there between approximately 1200 and 500 B.C. [16], and parts of the structure remain intact today. Many of the spaces at the site are too small for a human to crawl into and too tortuous to be explored with a camera on a stick, so we were invited to use our vine robot to explore and take video inside tight spaces at the site. The site contains hundreds of largely unexplored underground tunnels that can range in size from approximately 30 to 100 cm across and stretch up to hundreds of meters long. Exploration of these tunnels is important to the archeology team because they might lead to other underground rooms, in which objects of interest may be found, or they may themselves contain objects of interest. Additionally, mapping the tunnels might lead to insights about their purpose or significance to the people who made them. We used video and photos of the site as well as discussions with the archeology team to develop design requirements for the version of the vine robot deployed at the archeological site.

Summary of Design Requirements

The basic requirement for pneumatically everting vine robot design is that the soft robot body be made of a nonstretchable material that is flexible enough to be turned inside out at the tip and that is capable of containing pressurized air.

Our system is also teleoperated to allow the human operator to make decisions about how to proceed with navigation and exploration in unstructured environments. To achieve effective teleoperation, the robot's growth and steering must be controllable, and there must be an interface for the human operator to give control inputs. There must also be a way for the human operator to observe the position of the robot tip within its environment.

Additionally, our system must be capable of navigation and exploration tasks, which means it must be able to grow to a length useful for navigation, pass through small apertures,

Table 1. Design requirements and solutions for vine robot system.

Capability	Requirement	Solution for Competition	Solution for Archeology
Pneumatically everting vine robot	Flexible, not stretchable, airtight soft robot body material	Thin, airtight plastic	Thin, airtight fabric
Teleoperation	Controllable growth	Antagonistic growth control with motor and pressure regulator	Antagonistic growth control with motor and pressure regulator
	Controllable steering	Series pouch motor actuators controlled by pressure regulators	Series pouch motor actuators controlled by pressure regulators
	Human operator control interface	Flexible joystick	Flexible joystick
	Human operator situational awareness	Line of sight to robot tip	Camera at robot tip and display with real-time video feedback
Navigation/ exploration	Length	Soft robot body material stored on reel in robot base	Soft robot body material stored on reel in robot base
	Aperture navigation	Natural soft robot body shrinking; aperture width less than body diameter	Smooth, rounded camera cap; aperture width equals body diameter
	Body support	Lightweight body material	Lightweight body material
Usability in the field	Portability	Small soft robot body diameter to ensure portable air compressor can fill it	Small soft robot body diameter to ensure portable air compressor can fill it
	Mechanical robustness	Plastic soft robot body	Durable fabric soft robot body
	Electrical robustness	All electronics run off line power; all signals wired	All electronics run off line power; all signals wired
	Speed of movement	Fast pressure control, backdrivable motor	Fast pressure control, backdrivable motor
	Data recording	Not applicable	Camera at robot tip with video recording

Authorized licensed use limited to: Stanford University. Downloaded on April 11,2021 at 23:34:42 UTC from IEEE Xplore. Restrictions apply.

and support its own body weight when navigating vertically and over gaps in the floor of the environment.

Finally, our system must be usable in the field, which means that it must be portable, mechanically and electrically robust enough to last through its particular mission (a single competition run or a week of testing at the archeological site); able to move fast enough to be practically useful; and, for the case of the archeological application, able to record data taken during exploration.

Table 1 summarizes these design requirements along with the design solutions chosen for the two slightly different versions of the vine robot deployed in the two locations.

System Overview

We present here the design and control of a vine robot system that is portable, teleoperated using visual feedback from a camera at the tip, and not inherently limited in length. Figure 1 shows diagrams of the three main capabilities of the robot system: its ability to extend to an arbitrary length, to accommodate reversible steering using soft pneumatic actuators, and to transport a camera at the robot tip. Figure 2 shows the complete system, made up of the growing portion of the robot, the base station, and the human interface for controlling the robot. The following sections discuss in detail each component of the system. Table 2 lists the design specifications for the two versions of the robot, which will be explained as the appropriate components are discussed.

Mechanical Design

Soft Robot Body Design

The soft body of the vine robot is made of four airtight tubes that are flexible but not stretchable: one central main body tube and three smaller actuator tubes placed around the main body tube [Figure 1(a) and (b) and Figure 3(c)]. Growth is achieved by pressurizing the main body tube. One end of the main body tube is fixed to an opening in a rigid pressure vessel (Figure 4). The other end of the tube is folded inside itself and wrapped around a spool inside the pressure vessel. This allows a long length of robot body material to be stored in a compact space. Pressurizing the pressure vessel, and thus the main body tube, while allowing the body material to unroll from the spool causes the robot body to elongate from the tip.

Thin, airtight plastic was chosen for the competition robot body, because it could be purchased in a tube shape, which allowed rapid prototyping and manufacturing. Thin, airtight fabric was chosen for the archeological exploration robot body, because a more durable material was needed to withstand repeated use in the abrasive environment of the tunnels. Both materials are lightweight to allow the robot body to support its own weight.

The soft robot body length was chosen to be just long enough to complete the competition course or to achieve useful exploration at the archeological site. The soft robot body diameter was chosen to be large enough to allow growth at a low pressure [17] but small enough for the air compressor to quickly fill the robot body's increasing volume during growth. The diameter of the archeology robot was slightly larger than that of the competition robot, because the additional thickness of the fabric meant that a larger diameter was needed to grow at the same pressure.

Reversible steering of the robot body was achieved using the three actuator tubes, each of which was partially heat-sealed at regular intervals to create a series-pouch-motor soft pneumatic actuator that shortens when inflated (see Figure 3). These actuators are based on the pouch motors presented in [18] and are arranged in series like the series pneumatic artificial muscles presented in [11] and [13], yielding a design that is easily manufactured in long lengths and easily attached to the main body tube. We chose the actuator tube diameters to be as large as possible while allowing a small gap between neighboring actuators. The three series pouch motors were attached lengthwise to the exterior of the main body using double-sided tape (MD 9000, Marker-Tape, Mico, Texas), equally spaced around the circumference of the main body tube. When one of the series pouch motors is pressurized, the length change that it produces causes the entire robot to curve in the direction of that actuator [Figures 1(b) and 3(c)]. The three shortening actuators move the robot tip in two degrees of freedom (DoF) on a surface in 3D space. The third DoF of robot tip

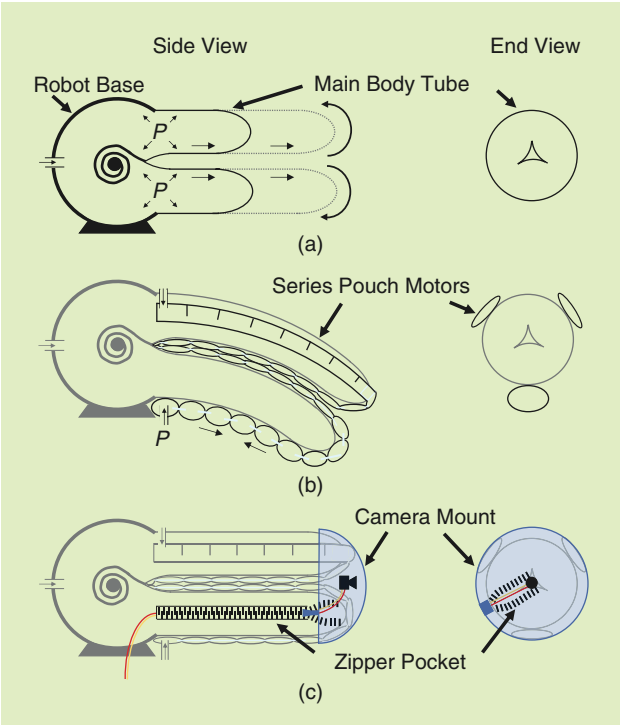

Figure 1. Diagrams showing three main features of our vine robot system: (a) Growth to an arbitrary length enabled by storing soft robot body material on a spool inside the robot base. (b) Reversible steering of the robot tip using series-pouch-motor soft pneumatic actuators that run the length of the robot body. (c) Transport of a wired camera at the robot tip using a rigid cap that is pushed along as the robot body grows, as well as a pocket that contains the camera wires running the length of the robot body; the pocket is zipped up as the body grows.

Authorized licensed use limited to: Stanford University. Downloaded on April 11,2021 at 23:34:42 UTC from IEEE Xplore. Restrictions apply.

Figure 2. The complete vine robot system. Components include the growing portion (which contains the soft robot body and camera mount), the base station (which contains the mechanical, electrical, and pneumatic components required to move the growing portion), and the human interface (which contains the flexible joystick and the display for viewing camera images).

Table 2. Design specifications for vine robot system.

Feature	Specification for Competition	Specification for Archeology
Soft robot body material	0.005-cm-thick low-density polyethylene (Uline, Pleasant Prairie, Wisconsin)	0.015-cm-thick thermoplastic polyurethane-coated ripstop nylon (Seattle Fabrics, Seattle, Washington)
Soft robot body length	10 m	7.5 m
Main body tube diameter	5 cm	7.5 cm
Actuator tube diameter	2.5 cm	3.7 cm
Robot base diameter	20 cm	30 cm
Robot base length	30 cm	30 cm
Maximum extension speed	10 cm/s	10 cm/s
Maximum extension pressure	14 kPa	21 kPa
Maximum steering pressure	14 kPa	21 kPa
Maximum air-compressor flow rate	470 cm^3/s	470 cm^3/s

motion is produced through growth. Growth and steering can occur simultaneously.

Base Station Design

Control of the vine robot body's motion is enabled by the mechanical, electrical, and pneumatic components of the base station. The robot base (see Figure 4), a cylindrical pressure vessel made by enclosing a large acrylic cylinder with two end caps (QC-108 or QC-112, Fernco, Davison, Michigan), is used to store the undeployed robot body material on a spool. A second, smaller cylinder is fixed inside a hole in the large cylinder using hot glue, and the base of the main body tube of the vine robot is clamped to this smaller cylinder to create an airtight seal. To allow the robot body to grow to full length and still be pulled back after deployment, the distal end of the main body tube is attached to a string the length of the robot body. The string is tied to the spool in the base. The spool is driven by a motor (CHM-2445-1M, Molon, Arlington Heights, Illinois) with an encoder (3081, Pololu, Las Vegas, Nevada), which allows controlled release of the robot body material during growth and assists with retraction of the robot body material back into the base. The length of the robot base was chosen to contain the motor and spool assembly,

Authorized licensed use limited to: Stanford University. Downloaded on April 11,2021 at 23:34:42 UTC from IEEE Xplore. Restrictions apply.

and the diameter of the base was chosen to contain the rolled up soft robot body. The base for the archeological exploration needed to be larger in diameter than the base for the competition so as to store the thicker soft robot body material.

In addition to the robot base, the base station includes pressure regulators, control circuitry, an air compressor, and a solenoid valve. Control of the air pressure in the four tubes of the robot body is achieved using four closed-loop pressure regulators (QB3TANKKZP10PSG, Proportion-Air, McCordsville, Indiana) as depicted in Figure 2. An Arduino Uno (Arduino, Turin, Italy), signal-conditioning circuitry, and a motor driver (DRI0002, DFRobot, Shanghai, China) control the voltages sent to the motor and pressure regulators. A portable air compressor (FS-MA1000B, Silentaire Technology, Houston, Texas) provides a continuous supply of compressed air to the system.

For the competition, we used an air compressor that was provided. It had the same maximum flow rate and also had a storage tank. A fail-closed solenoid valve (MME-31NES-D012, Clippard, Cincinnati, Ohio) sits in-line between the air compressor and the pressure regulators to allow quick release of all pressure in the system in case of emergency or power failure. One determining factor of the vine robot's maximum growth speed is the maximum flow rate of compressed air through the system. This is why high flow-rate pneumatic components were selected. The air compressor ended up being the component that limited the system's overall maximum flow rate. For robustness, all connections in the system are wired, and no part of the system runs on battery power. This allows continuous operation in the field, provided that power lines are available.

Flexible Joystick Design

We used a flexible joystick (first presented in [14]), adapted with additional control switches and potentiometers, as the interface for a human operator to teleoperate the vine robot. The mechanical design and components of the joystick are shown in Figure 5. The shape of the joystick mimics the long, thin, bendable shape of the soft body of the vine robot. For the operator, this makes steering more intuitive [14]. The joystick is made of 3D-printed flexible rubber (NinjaFlex, NinjaTek, Manheim, Pennsylvania). An inertial measurement unit (IMU) (EBIMU-9DOFV3, E2BOX, Hanam, South Korea) on the flexible joystick measures the orientation of the tip.

In addition to the IMU, which controls the steering of the vine robot, the flexible joystick contains inputs for main body pressure and motor speed, which together control growth (Figure 6). A rotary potentiometer sets the pressure in the main body, and a sliding potentiometer sets the desired motor speed. The joystick also includes an emergency-stop toggle switch.

Camera Mount Design

For the competition, the focus was on navigating the robot tip through the obstacles, and the operator was allowed

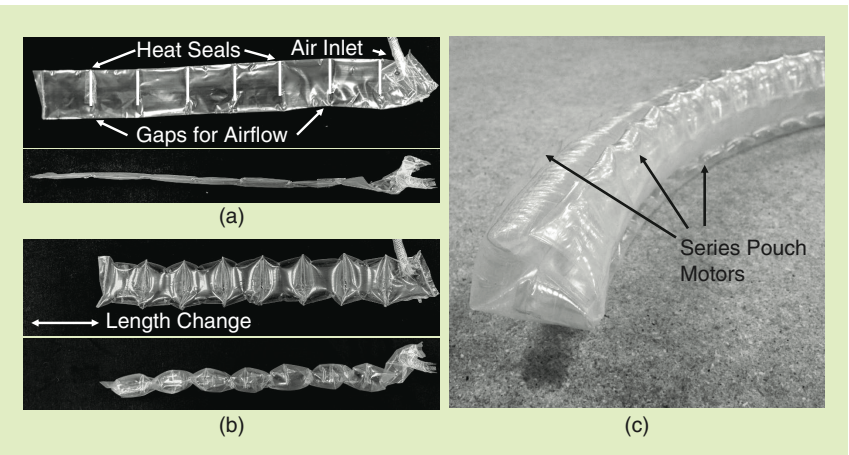

Figure 3. The soft actuation for steering the robot. (a) The top and side views of the deflated actuator, constructed by partially heat-sealing a tube of airtight, flexible material at regular intervals. (b) The top and side views of the inflated actuator, which balloons out at each pouch, causing shortening along the entire length. (c) A close-up of the vine robot tip, showing three series pouch motors spaced equally around the main body tube. One series pouch motor is inflated, causing the robot body to reversibly curve toward it.

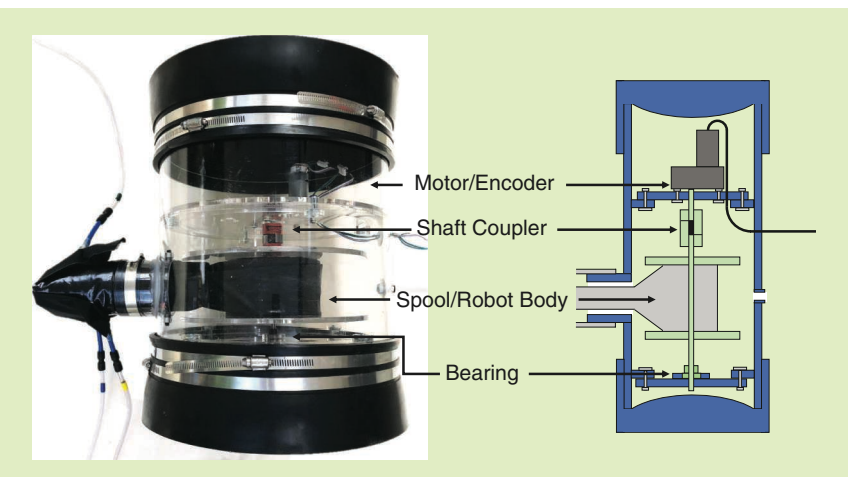

Figure 4. A photo and diagram illustrating the base from which the robot is extended and into which the robot retracts. The robot body material is stored inside a pressurized cylinder on a spool driven by a motor/encoder to control the speed of extension and aid in retraction.

Authorized licensed use limited to: Stanford University. Downloaded on April 11,2021 at 23:34:42 UTC from IEEE Xplore. Restrictions apply.

direct line of sight of the robot tip, so no camera was needed. However, for the archeological exploration, the focus was on exploration and data collection in an unknown environment, so we mounted a camera (HDE-SpyCamPro, Toronto, Canada) at the robot tip to allow teleoperation and video recording. The camera is mounted to a rigid cap, which stays at the robot tip during growth (Figure 7). The cap's inner diameter (10.4 cm) is slightly larger than the outer diameter of the soft robot body when one or two of the actuator tubes are inflated; this allows the cap to slide freely along the robot body and be pushed along by the robot tip as the robot grows. The bullet shape guides the cap as it slides along walls or past obstacles it touches from any angle. A strip of LED lights surrounds the camera to illuminate the environment in front of the robot. The camera has a wide-angle lens to allow it to capture approximately 120° of the environment without moving.

Since wireless signals are difficult to transmit underground, we used a wired camera for archeological exploration. The camera wire is stored coiled up at the base of the robot. As the soft robot body grows, the wire is pulled along the exterior of the robot body by the camera cap. To prevent the wire from snagging on the environment, a low-density polyethylene pocket on the soft robot body contains the camera wire and allows it to slide inside the pocket without directly contacting the environment. Using a zipper mechanism, the pocket lengthens as the soft robot body grows [Figures 1(c) and 7]. A zipper runs the entire length of the pocket, with the base of the zipper at the base of the robot. The zipper head is fixed to the camera cap so that the zipper starts out unzipped when the soft robot body is short and zips up as the robot grows, thus creating a pocket that is always the length of the soft robot body. The zipper also prevents rotation of the camera cap relative to the soft robot body, simplifying the mapping between movements of the camera image and actuators.

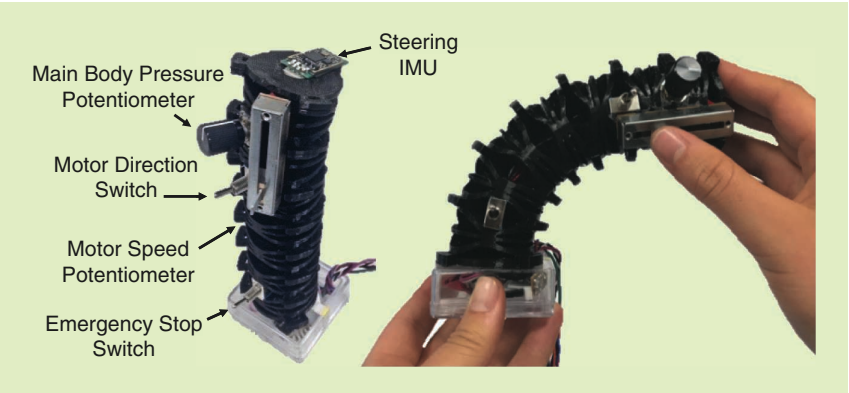

Figure 5. The flexible joystick used for teleoperation. The joystick contains switches and sensors to control the motion of the soft robot body.

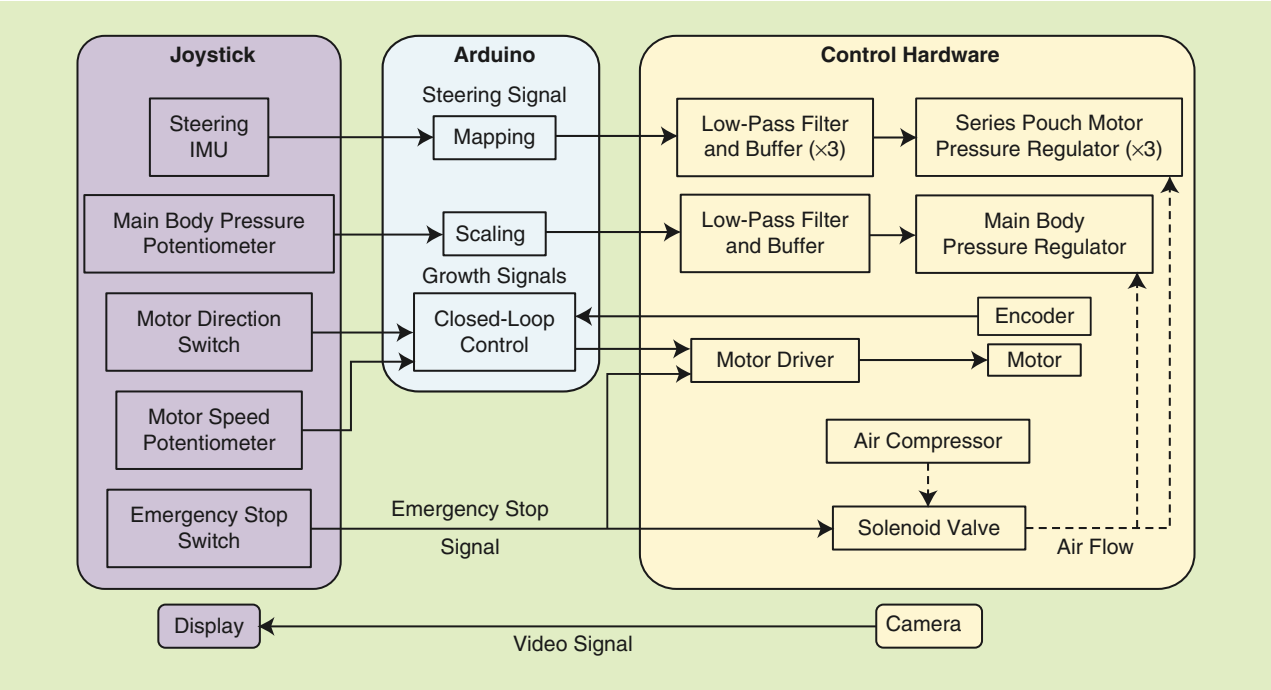

Figure 6. A diagram of the vine robot's electrical signals and air flow. The components of the human interface are shown in purple, the Arduino is shown in blue, and the components of the sensing and control hardware are shown in yellow. Electrical signals are shown with a solid line, and the flow of compressed air is shown with a dotted line.

Authorized licensed use limited to: Stanford University. Downloaded on April 11,2021 at 23:34:42 UTC from IEEE Xplore. Restrictions apply.

Control

Figure 6 shows the flow of information between the human interface and the sensing and control hardware of our vine robot system. This section describes in detail the mapping, scaling, and closed-loop control performed within the Arduino to convert joystick inputs into the motor voltage and the four pressures used to control the movement of the robot body. Growth and steering are controlled independently and occur simultaneously. Since we do not sense the robot shape, our controller relies on the human operator to close the loop via line-of-sight or camera feedback to achieve a desired robot tip position.

Growth Control

Growth is controlled by balancing the main body pressure with the motor voltage. The main body pressure is directly set using the main body pressure potentiometer as

$$p = c_p(r_p - r_{p0}), \tag{1}$$

where p is the desired pressure in the main body, c_p is a constant that converts units of potentiometer readings to units of pressure, r_p is the current potentiometer reading, and r_{p0} is the potentiometer reading at the position that corresponds to zero pressure. A closed-loop pressure regulator runs its own internal control loop to maintain a desired pressure given an analog voltage input. The Arduino pulsewidth modulation signal is sent through a low-pass filter and buffer to create a true analog voltage input for the pressure regulators.

The desired motor speed ω_d is commanded with the motor direction switch and motor speed potentiometer as

$$\omega_d = d\, c_m(r_m - r_{m0}), \tag{2}$$

where d equals −1 if the motor direction switch is in the growth direction and 1 if the motor direction switch is in the retraction direction, c_m is a constant that converts units of potentiometer readings to units of motor speed, r_m is the current potentiometer reading, and r_{m0} is the potentiometer reading at the position that corresponds to zero motor speed. The desired motor speed is maintained using a proportional–integral control loop based on readings from the encoder attached to the motor, and the motor voltage control signal u is calculated as

$$u = k_p(\omega_d - \omega) + k_i \int (\omega_d - \omega), \tag{3}$$

where k_p is the proportional control constant, k_i is the integral control constant, and ω is the actual motor speed as measured by the encoder.

Because only pressure can cause the robot to grow and only motor voltage can cause the robot to retract, a delicate balance must be maintained between pressure and motor voltage to ensure that growth is under control. For smooth growth to occur, the main body pressure must be higher than the pressure needed to grow [17], [19], and the motor must maintain tension in the robot body and/or string coming off the spool. If the motor spins faster in the growth direction than the robot is growing, the robot material or string will become slack, and the human operator will be unable to slow the growth. For this reason, we use a backdrivable motor to restrain the robot's growth. In our teleoperation controller, if the calculated motor voltage control signal would cause rotation and/or torque of the motor in the growth direction, the motor voltage is instead set to just cancel the Coulomb friction in the gearing of the motor. This allows the motor to be easily backdriven by the string or robot body and to unspool material when needed while never unspooling material too quickly. The maximum growth pressure used was 14 kPa for the competition robot and 21 kPa for the archeology robot, and the maximum observed growth speed for both systems was approximately 10 cm/s.

Using a zipper mechanism, the pocket lengthens as the soft robot body grows.

Steering Control

Steering control is achieved using the measured orientation of the IMU at the tip of the joystick to determine the desired position of the soft robot body tip within a shell defined by the two DoF of movement not governed by growth [11]. Movement of the robot tip to this position is then enacted in an open-loop fashion by setting the desired pressures of the three closed-loop pressure regulators that supply air to the three series-pouch-motor actuators.

First, the IMU-measured joystick tip orientation, q, represented in quaternion form, is used to calculate the curvature amount κ and the direction of curvature (i.e., bending plane angle) ϕ of the joystick. Based on the constant curvature

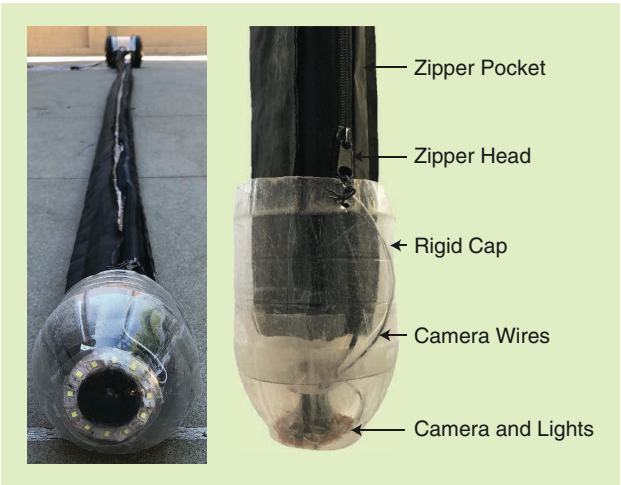

Figure 7. The camera mount system. The camera and lights are contained in a clear, rigid cap that is pushed along as the vine robot is extended. The camera wires are stored at the robot base and slide through a zipper pocket that extends with the robot.

Authorized licensed use limited to: Stanford University. Downloaded on April 11,2021 at 23:34:42 UTC from IEEE Xplore. Restrictions apply.

model of continuum robots [20], these shape parameters are calculated as

$$\kappa = \frac{\cos^{-1}(1 - 2(q_x^2 + q_y^2))}{s}, \kappa > 0,$$
$$\phi = \tan^{-1}\left(\frac{q_x q_w + q_y q_z}{q_x q_z - q_y q_w}\right), -\pi \le \phi < \pi, \tag{4}$$

where q_w and $[q_x, q_y, q_z]^T$ are the scalar and the vector components of $\boldsymbol{q}$, and s is the length of the flexible joystick. Then, the x and y coordinates of the 3D position of the joystick tip relative to its base are calculated using

$$x_{\text{joystick}} = -\frac{\cos(\phi)(\cos(\kappa s) - 1)}{\kappa},$$
$$y_{\text{joystick}} = \frac{\sin(\phi)(\cos(\kappa s) - 1)}{\kappa}. \tag{5}$$

Next, the desired robot tip coordinates are set equal to the current joystick tip coordinates, and the movement of the robot tip to these coordinates is enacted through setting the three series-pouch-motor pressures based on a simple geometric model of the soft robot body adapted from the geometric and static model presented in [11] and [13]. Pressurization of each series pouch motor is assumed to cause movement of the robot tip toward that series pouch motor with a displacement proportional to the pressure. The resulting position of the robot tip is assumed to be a superposition of the displacements produced by each series pouch motor, as

$$x = c(p_1 \cos(\psi_1) + p_2 \cos(\psi_2) + p_3 \cos(\psi_3)),$$
$$y = c(p_1 \sin(\psi_1) + p_2 \sin(\psi_2) + p_3 \sin(\psi_3)), \tag{6}$$

where c is a tunable constant that converts units of pressure into units of robot tip displacement and controls the amount of curvature enacted in the soft robot body for a given movement of the joystick; p_1, p_2, and p_3 are the pressures sent to the three series pouch motors; and ψ_1, ψ_2, and ψ_3 are the angles counterclockwise from the positive x-axis at which the three series pouch motors are placed around the circumference of the soft robot body. Due to the weight of the soft robot body, only the curvature of its most distal 1 m (approximately) can be controlled by the human operator, while the rest of its body tends to remain fixed. This results in approximately the same robot tip movement at various robot body lengths. The pressures sent to the actuators are calculated by solving (6) as

$$p_1 = \frac{\sin(\psi_3 - \psi_2)}{\sin(\psi_2 - \psi_1)} p_3 + \frac{x \sin(\psi_2) - y \cos(\psi_2)}{d \sin(\psi_2 - \psi_1)},$$
$$p_2 = \frac{\sin(\psi_3 - \psi_1)}{\sin(\psi_1 - \psi_2)} p_3 + \frac{x \sin(\psi_1) - y \cos(\psi_1)}{d \sin(\psi_1 - \psi_2)},$$
$$p_3 = p_3. \tag{7}$$

Since there are three actuators but only two DoF steering, there is a redundancy in the actuation, which we handle by always ensuring that the pressure in at least one of the actuators is close to zero. We start from an initial guess of zero for the value of p_3 and calculate p_1 and p_2. Then, we iteratively update the guess for p_3 and solve for p_1 and p_2 again until all of the calculated pressures are positive and at least one of the calculated pressures is within a small tolerance of zero. This avoids unnecessary shortening and stiffening of the robot body due to cocontraction of opposing series pouch motors. The maximum steering pressure used was 14 kPa for the competition robot and 21 kPa for the archeology robot.

Deployment at a Soft Robot Navigation Competition

Seven robots from around the world competed in the RoboSoft 2018 soft robot navigation competition. Figure 8 shows the vine robot successfully executing the four obstacles: the sand pit, square aperture, stairs, and unstable cylinders. The vine robot was the only robot in the competition to navigate all obstacles perfectly on the first attempt. It also passed through the smallest aperture overall, as well as the smallest aperture relative to its body size. However, robots that did not move their whole body through each obstacle lost points. Consequently, this robot, designed to leave part of its body behind, received half points on the first three obstacles, which placed it third overall.

During practice, we were consistently able to teleoperate the vine robot through the course in under 3 min (6 cm/s). The sandpit did not present a problem, since the vine robot, unlike typical robots that move along the ground, does not need to exert force on the environment to move straight. Due to the hollow, air-filled inside of the soft robot body, the robot was consistently able to shrink its diameter while passing through an aperture with a side length of 4 cm for a robot with a 7-cm diameter when all four tubes were inflated (yielding a body-shrinking ratio of 0.57:1); if it were any smaller, the robot body would buckle and/or slide along the wall instead of going through the aperture. The robot had no trouble traversing the stairs obstacle, since the actuators could provide enough curvature to grow over each step. The robot could pass through the unstable cylinders without knocking them over, due to its low center of gravity and gentle contact; but it always slid one out of the way, due to its inability to make a tight S-shaped curve without the environment holding its body in place.

At the competition, because one of the closed-loop pressure regulators had broken in transit, the main body tube pressure was controlled by hand. Additionally, because of a leak caused in transit, the device required a flow rate greater than the maximum the air compressor could deliver (470 cm^3/s). This caused the storage tank on the air compressor to empty three times during the competition run, requiring pausing of growth to wait for the tank to refill. Despite these (correctable) challenges, the robot was able to execute all four obstacles perfectly on the first try. The total time required to complete the course was 13 min and 28 s.

Deployment at an Archeological Site

Figure 9 shows a map of the archeological site as well as photos and simulations of the locations explored by the

Authorized licensed use limited to: Stanford University. Downloaded on April 11,2021 at 23:34:42 UTC from IEEE Xplore. Restrictions apply.

vine robot. Three locations were chosen to be explored by the vine robot due to their interest to the archeology community, difficulty to explore through other means, expected length (fewer than 10 m from a human-sized entry way), and ease of setting up the vine robot at the entrance. Overall, the robot was able to achieve access inside all three of the targeted locations and take video that could not have been recorded otherwise. In Location 1, the robot was able to navigate past a rock blockage [Figure 9(b), top]. In Location 2, the robot was able to round a 90° turn [Figure 9(c), top and bottom]. In Location 3, the robot was able to grow upwards into a vertical shaft

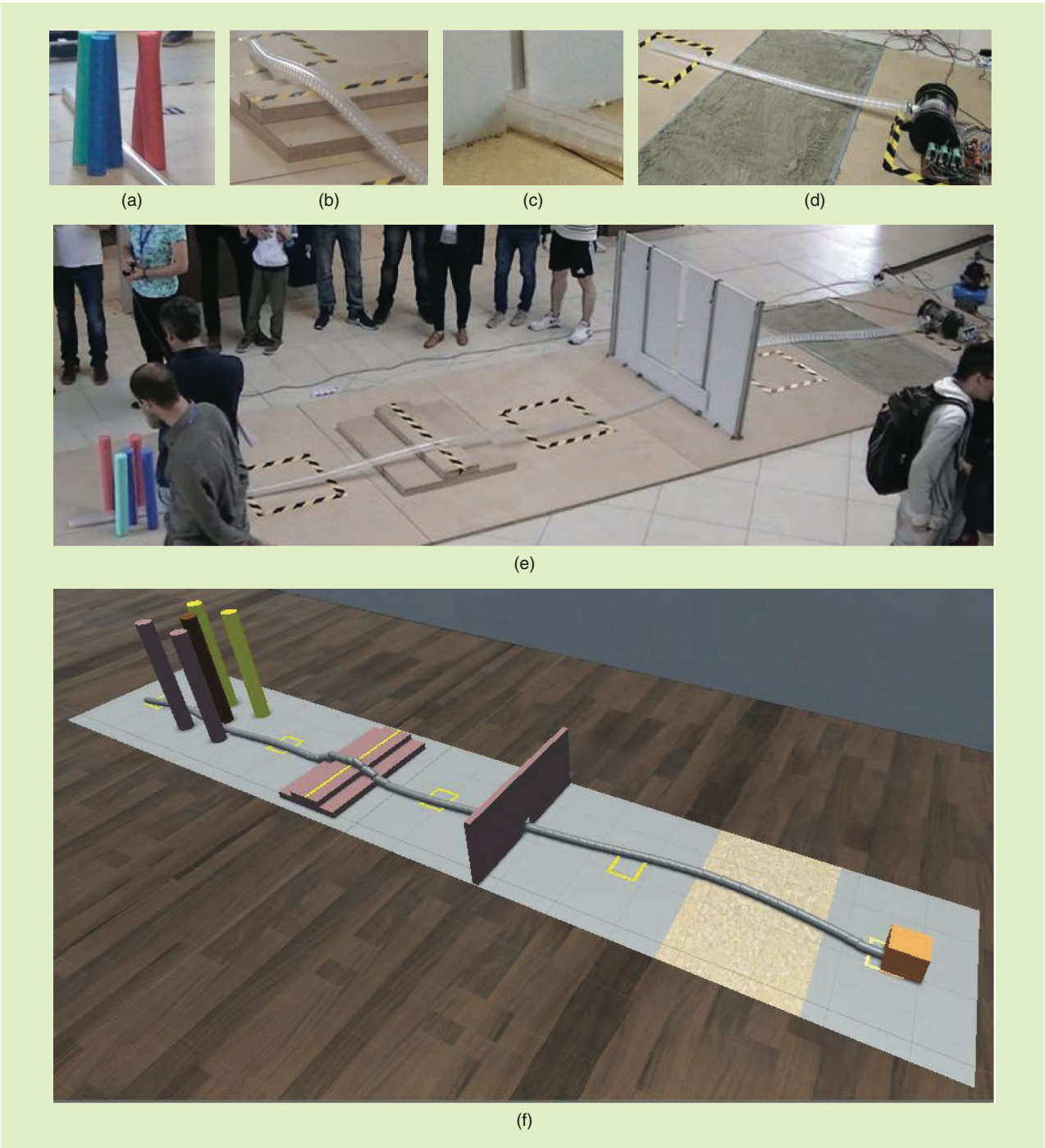

Figure 8. Photos and simulation images of the vine robot's successful completion of the RoboSoft 2018 soft robot navigation competition course, consisting of (a) unstable cylinders that were easily knocked over, (b) stairs, (c) a small aperture, and (d) a sand pit. (e) The vine robot after completing the entire competition course. (f) Simulation images of the vine robot's execution of the course. The vine robot was the only robot in the competition to navigate all obstacles perfectly on the first attempt. It also passed through the smallest aperture (4.5 × 4.5 cm) relative to its body size (7-cm diameter).

Authorized licensed use limited to: Stanford University. Downloaded on April 11,2021 at 23:34:42 UTC from IEEE Xplore. Restrictions apply.

Figure 9. The map, photos, and simulation images of the vine robot's successful exploration of underground tunnels in an archeological site in Chavin, Peru. (a) A map of the archeological site. Areas the vine robot explored are marked in purple. (b) Location 1: a tunnel nearly blocked by rocks. (c) Location 2: a tunnel with a 90° right-hand turn. (d) Location 3: a tunnel that slopes upwards and then turns vertically. Top row: photos from inside the tunnels; middle row: photos of the vine robot in the tunnels; bottom row: screenshots of the simulation of the vine robot in each tunnel.

Authorized licensed use limited to: Stanford University. Downloaded on April 11,2021 at 23:34:42 UTC from IEEE Xplore. Restrictions apply.

[Figure 9(d)]. The robot grew approximately 6, 5, and 3 m into each tunnel, respectively.

The challenges during this deployment of the robot were artificially slow growth speed, lack of actuator robustness, lack of shape morphing at the robot tip, inability to shorten the robot once grown, and difficulty maintaining situational awareness. First, growth was slower than it could have been because the length and narrowness of the chosen pressure tubing led to a significant unsensed pressure drop between the closed-loop pressure regulators and the soft robot body. Second, the heat seals on the actuators tended to pop open after repeated use, leading to leaks and an inability to curve the robot body. This was later improved by stapling over the heat seals and taping over the staples. Third, while the rigid camera cap at the robot tip enabled mounting and protected the camera, it also inhibited the vine robot's natural ability to pass along walls and squeeze through narrow apertures. This led to the need to push the robot forward from the base at some points. Fourth, due to the robot's natural tendency to buckle rather than reverse growth when the motor is run in the retraction direction, it was impossible to retract the robot while in the tunnels, resulting in the need to pull the robot back from the base to undo wrong turns and remove the robot after deployment. Fifth, challenges with situational awareness came from teleoperating the robot based only on the image from the tip camera. Because the tip of the robot body sometimes rolled relative to its base, changing the alignment of the camera image with gravity, the mental mapping between the bending directions of the joystick and the world-grounded directions in the tunnels was not always intuitive. Also, it was difficult to maintain an understanding of how far and in what direction the robot tip had gone, leading to confusion about the state of the robot and its environment. Even with these challenges, the vine robot gained access inside all three tunnels and recorded video in locations not previously observed by the archeology team.

Discussion and Future Work

In this article, we presented a complete vine robot system for use in the field for navigation and exploration tasks, and we reported on deployment of two slightly different versions of this system: the first to successfully navigate the RoboSoft 2018 soft robot navigation competition course and the second explore an archeological site in Chavin, Peru.

In the competition, the vine robot proved its ability to move over and around obstacles in a manner different from that of the other robots in the competition. Tasks that provided challenges for other robots, such as both passing through a small aperture and surmounting stairs, were easy for the vine robot. Its only disadvantage in the competition was the penalty that it incurred in the scoring due to its growth-based movement. This raises the point that there are some situations in which leaving behind part of the robot body is not ideal. In such cases, vine robots would not be the robot of choice. However, there are many scenarios in which the vine robot structure is advantageous, such as in cases where a conduit for fluids and electrical signals needs to be provided.

At the archeological site, the vine robot demonstrated its capability to navigate over rocks, around curves, and up vertical shafts, in each case having started from a compact form factor. Navigating the sandy and rocky terrain was easier for this robot than it likely would have been for locomoting robots that rely on exerting forces on the environment for movement. Meanwhile, this robot, compared to typical elongating continuum robots, appears to more easily fit into the small entrances and navigate the long and tortuous paths of the tunnels. However, due to the lack of direct line of sight to the robot tip, the robot was not as successful in exploring the archeological site as it was in completing the competition course. One question that remains open is how best to transport a camera or other sensors via a pneumatically everting vine robot without encumbering the robot's natural ability to morph its shape and grow along or over obstacles at its tip. In addition, we need to develop methods for retracting the vine robot without buckling. Finally, we wish to improve situational awareness for the human operator of a vine robot in an occluded environment where the operator does not have a direct line of sight to the robot tip.

The vine robot was the only robot in the competition to navigate all obstacles perfectly on the first attempt.

With the design of robust, field-ready vine robots, we aim to improve the state of the art for robots that can nondestructively explore small spaces. Continued research into burrowing with pneumatically everting vine robots [19] could open doors to navigation in even more restricted spaces than is currently possible. Additionally, using the vine robot's body as a conduit to pass material through it could take advantage of its unique mechanism of movement through growth.

Another goal of this project is to make the design of vine robots accessible for other researchers and end users. We created a website (https://www.vinerobots.org/) with step-by-step instructions for making pneumatically everting vine robots without active steering, and we will add designs and control software for other vine robot versions in the future.

Acknowledgments

We thank Marcello Calisti and Jamie Paik for organizing the RoboSoft 2018 competition; John Rick, Jack Lane, Daniel Chan, and the Stanford Global Engineering Program for supporting the vine robot's deployment at the archeological site; Jon Stingel and Tariq Zahroof for their contributions to the vine robot base design and teleoperation; and Joey Greer for useful discussions about vine robot growth control. This work was supported in part by the U.S. Air Force Office of Scientific Research grant FA2386-17-1-4658, the National Science Foundation grant

Authorized licensed use limited to: Stanford University. Downloaded on April 11,2021 at 23:34:42 UTC from IEEE Xplore. Restrictions apply.

1637446, and the project "Toward the Next Generation of Robotic Humanitarian Assistance and Disaster Relief: Fundamental Enabling Technologies (10069072)" funded by the Ministry of Trade, Industry and Energy of South Korea.

References

[1] Z. Liu and Y. Kleiner, "State of the art review of inspection technologies for condition assessment of water pipes," *Measurement*, vol. 46, no. 1, pp. 1–15, 2013.

[2] R. R. Murphy, S. Tadokoro, and A. Kleiner, "Disaster robotics," in *Springer Handbook of Robotics*. New York: Springer, 2016, pp. 1577–1604.

[3] R. H. Taylor, A. Menciassi, G. Fichtinger, P. Fiorini, and P. Dario, "Medical robotics and computer-integrated surgery," in *Springer Handbook of Robotics*. New York: Springer, 2016, pp. 1657–1684.

[4] O. Khatib et al. "Ocean One: A robotic avatar for oceanic discovery," *IEEE Robot. Autom. Mag.*, vol. 23, no. 4, pp. 20–29, 2016.

[5] M. B. Wooten and I. D. Walker, "A novel vine-like robot for in-orbit inspection," in *Proc. 45th Int. Conf. Environmental Systems*, 2015, pp. 1–11.

[6] M. Neumann and J. Burgner-Kahrs, "Considerations for follow-the-leader motion of extensible tendon-driven continuum robots," in *Proc. 2016 IEEE Int. Conf. Robotics and Automation (ICRA)*, pp. 917–923.

[7] A. Sadeghi, A. Mondini, and B. Mazzolai, "Toward self-growing soft robots inspired by plant roots and based on additive manufacturing technologies," *Soft Robotics*, vol. 4, no. 3, pp. 211–223, 2017.

[8] D. Mishima, T. Aoki, and S. Hirose, "Development of pneumatically controlled expandable arm for search in the environment with tight access," in *Field and Service Robotics*, S. Yuta, H. Asama, E. Prassler, T. Tsubouchi, and S. Thrun, Eds. Berlin: Springer, 2003, pp. 509–518.

[9] H. Tsukagoshi, N. Arai, I. Kiryu, and A. Kitagawa, "Tip growing actuator with the hose-like structure aiming for inspection on narrow terrain," *Int. J. Automation Technol.*, vol. 5, no. 4, pp. 516–522, 2011.

[10] E. W. Hawkes, L. H. Blumenschein, J. D. Greer, and A. M. Okamura, "A soft robot that navigates its environment through growth," *Sci. Robotics*, vol. 2, no. 8, p. eaan3028, 2017.

[11] J. D. Greer, T. K. Morimoto, A. M. Okamura, and E. W. Hawkes, "A soft, steerable continuum robot that grows via tip extension," *Soft Robotics*, pp. 95–108, 2018.

[12] J. Luong et al., "Eversion and retraction of a soft robot towards the exploration of coral reefs," in *Proc. 2019 2nd IEEE Int. Conf. Soft Robotics (RoboSoft)*, pp. 801–807.

[13] J. D. Greer, T. K. Morimoto, A. M. Okamura, and E. W. Hawkes, "Series pneumatic artificial muscles (sPAMs) and application to a soft continuum robot," in *Proc. IEEE Int. Conf. Robotics and Automation*, 2017, pp. 5503–5510.

[14] H. El-Hussieny et al., "Development and evaluation of an intuitive flexible interface for teleoperating soft growing robots," in *Proc. IEEE/RSJ Int. Conf. Intelligent Robots and Systems*, 2018, pp. 4995–5002.

[15] M. Calisti, M. Cianchetti, M. Manti, F. Corucci, and C. Laschi, "Contest-driven soft-robotics boost: The RoboSoft Grand Challenge," *Frontiers Robotics AI*, vol. 3, p. 55, 2016.

[16] S. R. Kembel and J. W. Rick, "Building authority at Chavin de Huantar: Models of social organization and development in the initial period and early horizon," in *Andean Archaeology*, H. Silverman, Ed. Malden, MA: Blackwell, 2004, pp. 51–76.

[17] L. H. Blumenschein, A. M. Okamura, and E. W. Hawkes, "Modeling of bioinspired apical extension in a soft robot," in *Conference on Biomimetic and Biohybrid Systems (Living Machines)*. New York: Springer, 2017, pp. 522–531.

[18] R. Niiyama, X. Sun, C. Sung, B. An, D. Rus, and S. Kim, "Pouch motors: Printable soft actuators integrated with computational design," *Soft Robotics*, vol. 2, no. 2, pp. 59–70, 2015.

[19] N. Naclerio, C. Hubicki, Y. Aydin, D. Goldman, and E. W. Hawkes, "Soft robotic burrowing device with tip-extension and granular fluidization," in *Proc. IEEE/RSJ Int. Conf. Intelligent Robots and Systems*, 2018, pp. 5918–5923.

[20] R. J. Webster, III and B. A. Jones, "Design and kinematic modeling of constant curvature continuum robots: A review," *Int. J. Robotics Res.*, vol. 29, no. 13, pp. 1661–1683, 2010.

Margaret M. Coad, Department of Mechanical Engineering, Stanford University, California. Email: mmcoad@stanford.edu.

Laura H. Blumenschein, Department of Mechanical Engineering, Stanford University, California. Email: lblumens@stanford.edu.

Sadie Cutler, Department of Mechanical and Aerospace Engineering, Cornell University, Ithaca, New York. Email: sc3236@cornell.edu.

Javier A. Reyna Zepeda, Department of Mechanical Engineering, Stanford University, California. Email: jreynaza@gmail.com.

Nicholas D. Naclerio, Department of Mechanical Engineering, University of California Santa Barbara. Email: nnaclerio@ucsb.edu.

Haitham El-Hussieny, Electrical Engineering Department, Faculty of Engineering (Shoubra), Benha University, Egypt. Email: haitham.elhussieny@feng.bu.edu.eg.

Usman Mehmood, School of Mechanical Engineering, Korea University of Technology & Education, Cheonan City, Chungnam Province. Email: usman.mehmood18@gmail.com.

Jee-Hwan Ryu, Department of Civil and Environmental Engineering, Korea Advanced Institute of Science and Technology, Daejeon. Email: jhryu@kaist.ac.kr.

Elliot W. Hawkes, Department of Mechanical Engineering, University of California Santa Barbara. Email: ewhawkes@ucsb.edu.

Allison M. Okamura, Department of Mechanical Engineering, Stanford University, California. Email: aokamura@stanford.edu.

Authorized licensed use limited to: Stanford University. Downloaded on April 11,2021 at 23:34:42 UTC from IEEE Xplore. Restrictions apply.